High Resolution Spectroscopy of the ν_5 Band of Fluoroform-d (CDF_3) by the Laser Stark Method

E. Ibisch and U. Andresen

Abteilung Chemische Physik im Institut für Physikalische Chemie, Universität Kiel

Z. Naturforsch. **35a**, 1020–1029 (1980); received July 19, 1980

The ν_5 perpendicular band of CDF_3 has been studied by means of laser Stark spectroscopy using the 10.4 μm band of the $^{12}C^{16}O_2$ and the $^{12}C^{18}O_2$ laser as infrared radiation sources. The assignment was established for more than 500 resonances. The majority of them was measured in saturation dip technique. A least-squares analysis of the Stark spectrum, together with recent microwave and infrared results, gave the rotation-vibration parameters and the dipole moment of the ν_5 state. A brief description of the apparatus is also given.

1. Introduction

Laser Stark spectroscopy with fixed-frequency lasers like CO_2, N_2O and CO lasers has shown to be a very powerfull tool to investigate rotation-vibration spectra of gaseous molecules. This results from the fact that these light sources are very monochromatic and their absolute frequencies are known to a high accuracy. The power of these lasers is usually strong enough to saturate the molecular transitions and thus to observe nonlinear effects like Lamb dip or level crossing. Solid state infrared detectors allow the detection of weak transitions with high sensitivity. This method has been applied to several molecules [1–12] primarily symmetric top rotors.

In the present paper we report the application to the ν_5 band of deutero-fluoroform (CDF_3). The IR spectrum of CDF_3 was first reported by Polo and Wilson [13], later by Hoskins [14], Ruoff et al. [15–17] and Fyke et al. [18]. The microwave spectra in the ground and several excited states have been investigated by Ghosh et al. [19] and mainly by Costain [20]. The ground state constants except the centrifugal distortion constants are given with high precision by Meerts and Ozier [21] from molecular beam experiments.

The 10.4 μm emission bands of the $^{12}C^{16}O_2$ and $^{12}C^{18}O_2$ lasers overlap most of the ν_5 band of CDF_3. Several near coincidences are found mostly with $^{12}C^{18}O_2$ laser lines. More than 500 Stark shifted molecular transitions are observed which allowed an accurate determination of the molecular parameters of the excited state.

Reprint request to Dr. U. Andresen, Abt. Chemische Physik, Institut für Physikalische Chemie, Universität Kiel, Olshausenstr. 40–60, D-2300 Kiel.

2. Experimental Details

A block diagram of the apparatus is given in Figure 1. The laser cavity of 2.8 m lenght is made of a plane grating (100 grooves/mm, blased at 10.6 μm) and a partly transmitting concave germanium mirror. The reflectivity is 80% except for low gain laser lines for which a similar mirror of 90% reflectivity is used. The laser gain tube, equipped with a water-cooling jacket, is 1.7 m long with 18 mm ID and sealed with ZnSe windows at Brewster angle. The tube is semi-sealed off, which

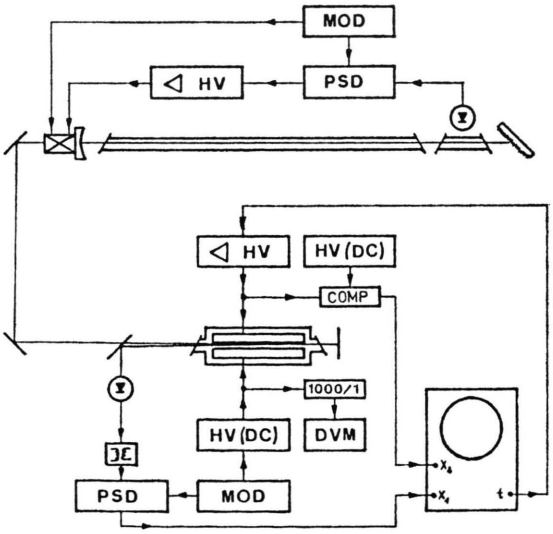

Fig. 1. Block diagram of the spectrometer. The apparatus is shown in saturation dip set up.

0340-4811 / 80 / 1000-1020 $ 01.00/0. — Please order a reprint rather than making your own copy.

allows also the economic use of $C^{18}O_2$ and $^{13}CO_2$ mixtures as a laser gas.

The output frequency of the laser is stabilized using the Lamb dip in the 4.3 μm CO_2 fluorescence radiation [22, 23]. The feed back loop consists of the fluorescence cell, the photoconductive In Sb detector (Valvo RPY 31), a lock-in amplifier (Ithaco 391 A), a HV amplifier and the piezoelectric translator (Lansing) carrying the concave mirror. A sine wave modulation of 0.5—1.4 kHz is applied to the translator to gain sensitivity by phase sensitive detection of the 4.3 μm radiation. With this feed back loop the line width of the laser frequency is in the order of 150 kHz [24]. The stabilisation is used commonly throughout all experiments.

The Stark cell consists of two stainless steel plates (40 × 10 cm) grounded flat to ± 0.5 μm. The plates are separated by ten precision-ground quartz spacers whose nominal thickness is 1 mm. For calibration we observed the QQ1(1) * and the QQ2(2) * transitions in the ν_3 band of methylfluoride (CH_3F). Using the parameters of Freund et al. [3] this leads to an effective plate spacing of 0.104 278(8) cm.

A DC voltage up to 6 kV from a high voltage power supply (Heinzinger HN 6000-10) is supplied to one plate superposed by a 10 kHz square wave voltage for modulation. The plate voltage is read out directly at a digital voltmeter after being fed into a voltage divider (Fluke 80 E). The other plate is connected to a high voltage DC amplifier (Kepco OPS 2000 A) which produces a ramp up to 2 kV for varying the Stark field. The ramp voltage is compared to a stable DC power supply (Fluke 415 B) using a zero-crossing detector.

The laser radiation is detected by a liquid-nitrogen cooled PbSnTe detector (Barnes). The output is impedance matched and fed directly into a phase sensitive detector (PAR Mod. 128 A). The obtained signal is displayed on an oscilloscope or recorded on an XY-recorder as the first derivative of the absorption line.

Two samples of CDF_3 were used in the course of the measurements, one supplied by Merck, Sharp and Dohme (Canada) with 99% purity and one synthetized in our laboratory. The sample was obtained in the following way. A small autoclave filled with 0.035 mole pure silver-fluoride (AgF) was cooled down to liquid nitrogen temperature and evacuated. After adding of 0.011 mole deuterobromoform ($CDBr_3$) the autoclave was closed and slowly heated to 180 °C at 2.5 atm pressure. After a reaction time of 1/2 hour CDF_3 was obtained which was purified by fractionated destillation.

The spectra were recorded with parallel polarization of the Stark field with both the $^{12}C^{16}O_2$ and the $^{12}C^{18}O_2$ lasers. The sample pressure was in the range of 7—20 mTorr and Stark fields up to 70 kV/cm were applied without discharge. The square wave modulation was 0.5—1.5 V for saturation dip spectra and 5—10 V for Doppler limited spectra.

3. Observed Spectrum

For an overview a Fourier transform spectrum of the CF_3 rocking vibration (ν_5) was recorded. Using a Digital Mod FTS-20 spectrometer a resolution of 0.07 cm^{-1} was obtained, which does not allow to resolve single lines of the band. Since in literature three values for the band centre were given [14, 15, 18] a more precise determination was carried out. The partial band contour analysis of the spectrum leads to a value of 975.42 ± 0.01 cm^{-1} [25].

Thus the band origin is located between the 10 R 18 * and 10 R 20 laser lines and many of the 10.4 μm band laser lines of both the $^{12}C^{16}O_2$ and $^{12}C^{18}O_2$ lasers could be used to observe Stark shifted resonances.

In a first run we recorded the Doppler limited spectrum. It appears as many strong and broad features with only very few clearly recognizable P/R series **. Figures 2 and 3 give some examples. To resolve those features it was necessary to record also the saturation dip spectrum. Figures 2 b and 3 b give an appropriate example.

For assignment we use a) the relative intensity and relative spacing of consecutive resonances of the series and b) the sign and magnitude of the Stark coefficient $s = \partial \nu_M(E)/\partial E$ (E is the electric Stark field and $\nu_M(E)$ is the molecular transition frequency at this field). To obtain the Stark coefficient s, we shifted the laser frequency by slightly changing the resonator length with laser stabilisa-

* For explanation see caption of Table 2.

* 10 R 18 denotes the R 18 line in the 10.4 μm band of the $^{12}C^{16}O_2$ laser while lines referring to the $^{12}C^{18}O_2$ laser are given as 10 R 18 (18 O).

** "Series" denotes sets of Stark shifted transitions all originate from the same rovibronic transition.

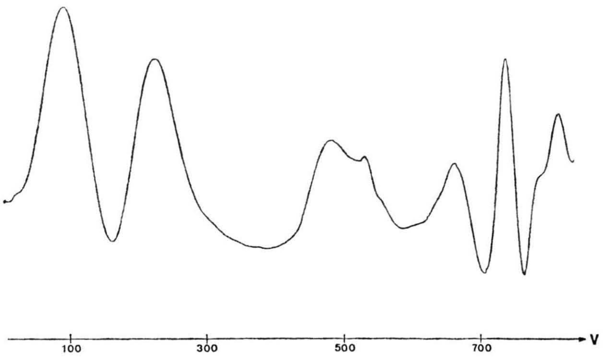

Fig. 2. Part of the spectrum of CDF_3 using the 10 R 16 laser line.

a) Doppler limited spectrum, sample pressure: 10 mT; modulation: 8 Vpp, 10 kHz; time constant for detection: 100 msec.

b) saturation dip spectrum of the same range. The M-components of the two Q-branch transitions are marked; sample pressure: 8 mT; modulation 1 Vpp, 10 kHz; time constant for detection: 100 msec.

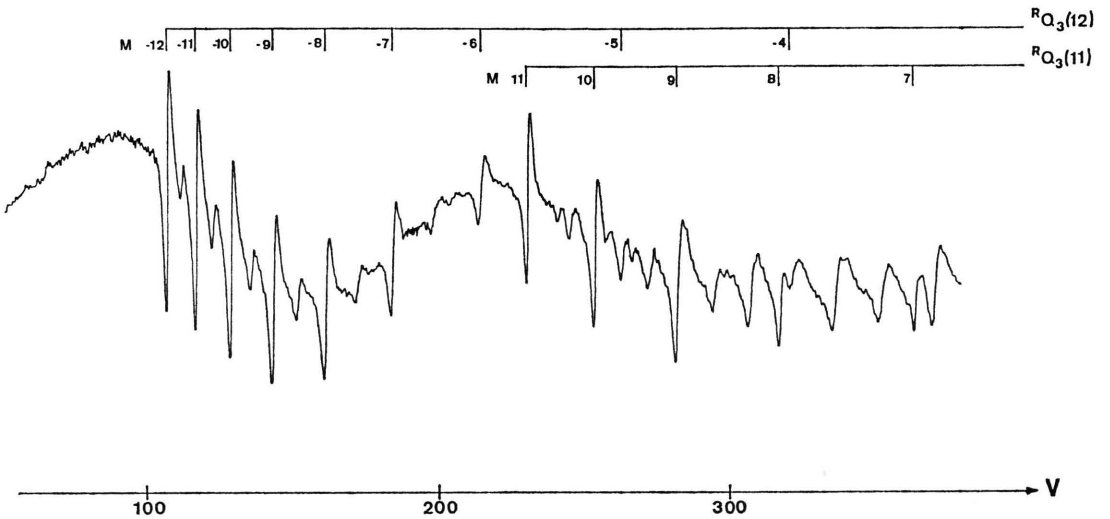

tion off. In nearly all cases the sign of s is the same as the sign of the difference between the laser and the zero-field transition frequency $\nu_L - \nu_M$ (ν_L laser frequency).

In Table 1 all assigned Stark shifted transitions are listed. The given transition frequencies at the indicated field are calculated using the derived parameters in Table 3. The laser frequencies are those reported by Petersen et al. [26] and by Freed et al. [27]. Table 2 shows the corresponding zero-field transition frequencies and the differences to the appropriate laser line.

4. Analysis

The Hamiltonian used for the analysis is given by [28, 29]

$$H = H_0 + H_l + H_s . \qquad (1)$$

H_0 denotes the rotational energy corrected for centrifugal distortion and H_s the Stark energy. Since the ν_5 vibrational state is a degenerate E state, the Coriolis splitting and the l-type doubling interaction has to be considered which is denoted by H_l. Only the first order Coriolis interaction and the ($\Delta k = \pm 2$, $\Delta l = \pm 2$) interaction [29] is explicitly included. All other higher order rotation-vibration interactions were neglected. We also ignored the J, k dependence of the dipole moment and the contributions to the Stark effect from the vibration induced dipole moment and the polarizability anisotropy.

The following matrix elements are explicitly considered for the excited state in units of $\hbar$:

$$\langle J, k, l, M | H_0 | J, k, l, M \rangle = \nu_5{}^0 + B' J(J+1) + (C' - B') k^2 - D_J' J^2 (J+1)^2 - D'_{JK} J(J+1) k^2 - D'_K k^4 , \qquad (2)$$

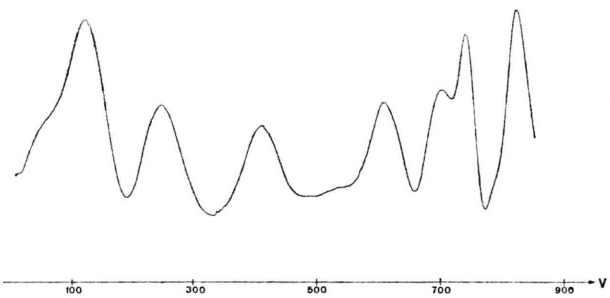

Fig. 3. Part of the spectrum of CDF_3 using the 10 R 22 laser line.

a) Doppler limited spectrum.

b) saturation dip spectrum. Experimental details see Figure 2.

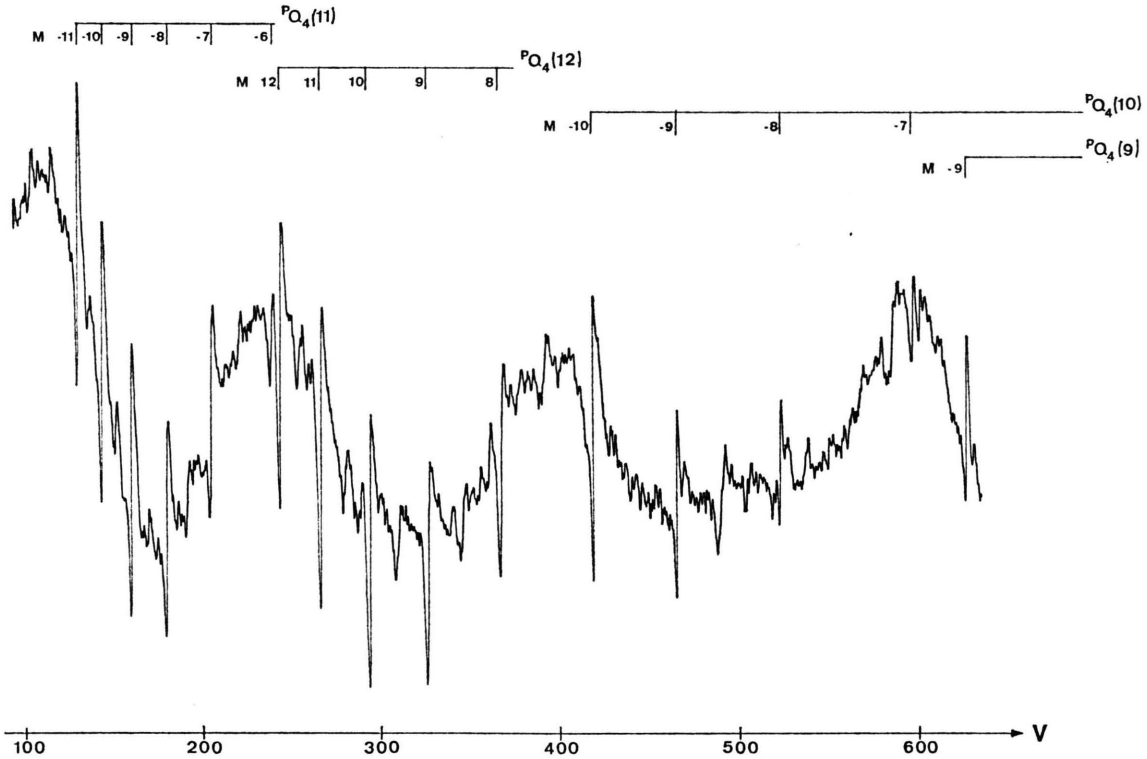

$$\langle J, k, l, M \,|\, H_l \,|\, J, k, l, M \rangle = -\,k\,l\,[2\,(C'\,\xi)_5 - \eta_J\,J\,(J+1) - \eta_K\,k^2]\,, \tag{3}$$

$$\langle J, k, l, M \,|\, H_l \,|\, J, k \pm 2, l \pm 2, M \rangle = 2\,q_5 \cdot \sqrt{[J\,(J+1) - k\,(k-1)][J\,(J+1) - (k-1)\,(k-2)]}\,, \tag{4}$$

$$\langle J, k, l, M \,|\, H_{\mathrm{S}} \,|\, J, k, l, M \rangle = -\,\mu'\,E\,k\,M / J\,(J+1)\,, \tag{5}$$

$$\langle J, k, l, M \,|\, H_{\mathrm{S}} \,|\, J-1, k, l, M \rangle = -\,\mu'\,E \sqrt{\frac{(J^2 - k^2)\,(J^2 - M^2)}{J^2\,(2\,J-1)\,(2\,J+1)}}\,. \tag{6}$$

In these expression $\nu_5{}^0$ is the frequency of the band centre; C' and B' are the rotational constants; D'_J, D'_{JK} and D'_K are the centrifugal distortion constants; $(C'\xi)_5$ is the Coriolis coupling constant; η_J and η_K are centrifugal corrections to the Coriolis coupling; q_5 is the l-type doubling constant; μ' is the dipole moment and E is the applied Stark field. J is the quantum number of the total angular momentum, $k = -J, -J+1, \ldots, J$ is the projection of the rotational angular momentum and $l = -v, -v+2, \ldots, v$ the projection of the vibrational angular momentum with respect to the symmetry axis of the rotor and v is the vibrational quantum number.

Table 1a. Observed Stark shifted transitions using the $^{12}C^{16}O_2$ laser lines. Only a fraction of these transitions were included laser lines and its frequencies are given as headline.

J"	K"	M"	J'	K'	M'	FIELD V/CM	VM(E) MHZ	VM(E)-VL MHZ
10R 4	28923046.4 MHZ					964.76898 CM-1		
13	3	-11	12	4	-11	30864	28923108.4	62.0
13	3	-10	12	4	-10	33912	28923105.3	58.8
13	3	-9	12	4	-9	37660	28923103.7	57.3
13	3	-8	12	4	-8	42292	28923098.7	52.3
10R 6	28967457.1 MHZ					966.25036 CM-1		
10	4	-9	9	5	-9	25064	28967402.3	-54.8
10	4	-8	9	5	-8	28236	28967402.7	-54.3
10	4	-7	9	5	-7	32264	28967395.7	-61.4
10	4	-6	9	5	-6	37753	28967396.3	-60.8
10R 8	29011133.0 MHZ					967.70723 CM-1		
11	0	-9	10	1	-9	2992	29011176.4	43.4
11	0	-8	10	1	-8	3356	29011176.0	43.0
11	0	-7	10	1	-7	3835	29011176.0	43.0
11	0	-6	10	1	-6	4480	29011176.3	43.3
11	0	-5	10	1	-5	5360	29011175.9	42.9
11	0	-4	10	1	-4	6673	29011175.4	42.4
11	0	-3	10	1	-3	8874	29011175.4	42.4
11	0	-2	10	1	-2	13221	29011175.4	42.4
10R10	29054072.7 MHZ					969.13955 CM-1		
8	1	3	7	2	3	732	29054110.6	37.9
8	1	2	7	2	2	1088	29054110.9	38.3
8	1	1	7	2	1	2100	29054112.4	39.7
7	2	6	6	3	6	17895	29054094.0	21.3
7	2	5	6	3	5	21401	29054097.5	24.9
7	2	4	6	3	4	26615	29054100.5	27.8
7	2	3	6	3	3	35422	29054076.7	4.0
6	3	5	5	4	5	24690	29054058.4	-14.3
6	3	4	5	4	4	30408	29054069.1	-3.6
10R16	29178455.7 MHZ					973.28852 CM-1		
15	3	-15	15	4	-15	15895	29178447.8	-7.9
15	3	-14	15	4	-14	17046	29178448.5	-7.2
15	3	-13	15	4	-13	18356	29178448.3	-7.4
15	3	-12	15	4	-12	19906	29178449.0	-6.7
15	3	-11	15	4	-11	21720	29178449.0	-6.7
15	3	-10	15	4	-10	23925	29178449.8	-5.8
14	3	-14	14	4	-14	9963	29178447.3	-8.4
14	3	-13	14	4	-13	10741	29178447.9	-7.8
14	3	-12	14	4	-12	11649	29178448.4	-7.3
14	3	-11	14	4	-11	12717	29178448.7	-7.0
14	3	-10	14	4	-10	13983	29178448.3	-7.3
14	3	-9	14	4	-9	15554	29178448.8	-6.9
14	3	-8	14	4	-8	17501	29178448.6	-7.0
13	3	-13	13	4	-13	5022	29178447.8	-7.8
13	3	-12	13	4	-12	5448	29178448.2	-7.4
13	3	-11	13	4	-11	5945	29178448.3	-7.4
13	3	-10	13	4	-10	6546	29178448.5	-7.1
13	3	-9	13	4	-9	7285	29178449.0	-6.7
13	3	-8	13	4	-8	8193	29178448.8	-6.9
12	3	-12	12	4	-12	1007	29178449.9	-5.8
12	3	-11	12	4	-11	1099	29178450.0	-5.7
12	3	-10	12	4	-10	1212	29178450.1	-5.6
12	3	-9	12	4	-9	1349	29178450.2	-5.5
12	3	-8	12	4	-8	1519	29178450.3	-5.4
12	3	-7	12	4	-7	1741	29178450.4	-5.2
12	3	-6	12	4	-6	2030	29178450.4	-5.3
11	3	11	11	4	11	2162	29178453.1	-2.5
11	3	10	11	4	10	2379	29178453.1	-2.6
11	3	9	11	4	9	2649	29178452.7	-2.9
11	3	8	11	4	8	2986	29178452.4	-3.3
11	3	7	11	4	7	3415	29178452.3	-3.4
11	3	6	11	4	6	3972	29178452.7	-3.0
11	3	5	11	4	5	4776	29178452.3	-3.3
10	3	10	10	4	10	4601	29178454.2	-1.4
10	3	9	10	4	9	5115	29178453.9	-1.7
10	3	8	10	4	8	5758	29178453.6	-2.0
10	3	7	10	4	7	6581	29178453.5	-2.2
10	3	6	10	4	6	7681	29178453.1	-2.6
10	3	5	10	4	5	9206	29178453.2	-2.5
10R16	29178455.7 MHZ					973.28852 CM-1		
9	3	9	9	4	9	6350	29178454.8	-0.8
9	3	8	9	4	8	7146	29178454.4	-1.2
9	3	7	9	4	7	8159	29178454.6	-1.0
9	3	6	9	4	6	9516	29178454.3	-1.4
8	3	8	8	4	8	7469	29178455.6	-0.1
8	3	7	8	4	7	8530	29178455.5	-0.2
8	3	6	8	4	6	9958	29178454.1	-1.5
8	3	5	8	4	5	11919	29178454.5	-1.2
7	3	7	7	4	7	8012	29178457.8	2.1
7	3	6	7	4	6	9347	29178456.5	0.8
7	3	5	7	4	5	11200	29178455.5	-0.1
7	3	4	7	4	4	13934	29178455.5	-0.2
6	3	6	6	4	6	8074	29178458.7	3.0
6	3	5	6	4	5	9675	29178457.1	1.4
6	3	4	6	4	4	12043	29178455.7	0.1
5	3	5	5	4	5	7719	29178457.8	2.2
5	3	4	5	4	4	9587	29178458.0	2.3
4	3	4	4	4	4	6984	29178459.4	3.7
4	3	3	4	4	3	9158	29178462.0	6.4
10R18	29218430.7 MHZ					974.62194 CM-1		
4	4	-3	3	3	-3	3279	29218402.6	-28.1
4	4	-2	3	3	-2	4996	29218404.3	-26.4
4	4	-1	3	3	-1	10692	29218403.4	-27.3
10R22	29296136.4 MHZ					977.21392 CM-1		
16	4	16	16	3	16	26484	29296124.1	-12.3
16	4	15	16	3	15	28193	29296121.8	-14.5
16	4	14	16	3	14	30247	29296123.8	-12.6
16	4	13	16	3	13	32582	29296124.6	-11.8
15	4	15	15	3	15	18787	29296122.1	-14.2
15	4	14	15	3	14	20142	29296123.0	-13.4
15	4	13	15	3	13	21682	29296122.8	-13.6
15	4	12	15	3	12	23487	29296123.0	-13.4
15	4	11	15	3	11	25626	29296123.5	-12.8
14	4	14	14	3	14	12248	29296121.3	-15.0
14	4	13	14	3	13	13206	29296122.3	-14.1
14	4	12	14	3	12	14312	29296122.7	-13.7
14	4	11	14	3	11	15600	29296122.3	-14.1
14	4	10	14	3	10	17168	29296122.8	-13.5
14	4	9	14	3	9	19054	29296122.4	-14.0
13	4	13	13	3	13	6786	29296121.6	-14.7
13	4	12	13	3	12	7357	29296122.0	-14.4
13	4	11	13	3	11	8014	29296121.5	-14.9
13	4	10	13	3	10	8826	29296122.0	-14.4
13	4	9	13	3	9	9811	29296122.3	-14.1
13	4	8	13	3	8	11048	29296122.8	-13.5
12	4	12	12	3	12	2286	29296120.8	-15.6
12	4	11	12	3	11	2504	29296121.3	-15.0
12	4	10	12	3	10	2758	29296121.5	-14.8
12	4	9	12	3	9	3070	29296121.8	-14.6
12	4	8	12	3	8	3463	29296122.2	-14.2
11	4	-11	11	3	-11	1244	29296123.9	-12.5
11	4	-10	11	3	-10	1369	29296123.8	-12.5
11	4	-9	11	3	-9	1525	29296123.6	-12.7
11	4	-8	11	3	-8	1716	29296123.6	-12.8
11	4	-7	11	3	-7	1961	29296123.7	-12.7
10	4	-10	10	3	-10	3953	29296126.8	-9.6
10	4	-9	10	3	-9	4399	29296126.4	-9.9
10	4	-8	10	3	-8	4956	29296126.1	-10.3
10	4	-7	10	3	-7	5674	29296125.6	-10.7
10	4	-6	10	3	-6	6630	29296125.4	-11.0
9	4	-9	9	3	-9	5944	29296126.9	-9.5
9	4	-8	9	3	-8	6696	29296126.5	-9.9
9	4	-7	9	3	-7	7666	29296125.9	-10.5
9	4	-6	9	3	-6	8974	29296124.8	-11.6
8	4	-8	8	3	-8	7252	29296126.6	-9.8
8	4	-7	8	3	-7	8287	29296127.3	-9.1
8	4	-6	8	3	-6	9693	29296126.5	-9.9
8	4	-5	8	3	-5	11662	29296126.2	-10.1

in the fit (see text).VM(E) Frequency of the M-component at the indicated field. VL Frequency of the laser line. The

J"	K"	M"	J'	K'	M'	FIELD V/CM	VM(E) MHZ	VM(E)-VL MHZ
10R22	29296136.4 MHZ					977.21392 CM-1		
7	4	-7	7	3	-7	7921	29296128.6	-7.7
7	4	-6	7	3	-6	9270	29296127.5	-8.9
7	4	-5	7	3	-5	11169	29296126.5	-9.9
7	4	-4	7	3	-4	14040	29296126.2	-10.2
6	4	-6	6	3	-6	8065	29296129.2	-7.1
6	4	-5	6	3	-5	9693	29296130.8	-5.6
6	4	-4	6	3	-4	12248	29296126.3	-10.0
10R26	29370829.6 MHZ					979.70542 CM-1		
7	1	7	8	2	7	10306	29370848.1	18.5
7	1	6	8	2	6	11925	29370851.1	21.5
7	1	5	8	2	5	14266	29370850.1	20.5
7	1	4	8	2	4	17510	29370855.5	25.9
6	0	-6	7	1	-6	25180	29370882.7	53.1
6	0	-5	7	1	-5	30460	29370886.9	57.3
6	0	-4	7	1	-4	38291	29370871.7	42.1
6	0	-3	7	1	-3	52734	29370884.1	54.5
10R28	29407038.2 MHZ					980.91321 CM-1		
8	0	8	9	1	8	11299	29407048.0	9.7
8	0	7	9	1	7	12902	29407047.7	9.4
8	0	6	9	1	6	15025	29407047.5	9.3
8	0	5	9	1	5	17968	29407047.7	9.4
8	0	4	9	1	4	22141	29407054.4	16.2
8	0	3	9	1	3	29312	29407050.1	11.9
7	1	7	8	0	7	19579	29407067.6	29.4
7	1	6	8	0	6	22837	29407064.1	25.9
7	1	5	8	0	5	27476	29407064.5	26.2
7	1	4	8	0	4	34521	29407065.8	27.5
6	2	6	7	1	6	32411	29407043.3	5.1
6	2	5	7	1	5	38824	29407040.4	2.1
6	2	4	7	1	4	48503	29407049.0	10.8
5	3	5	6	2	5	35326	29407039.8	1.5
5	3	4	6	2	4	43600	29407038.1	-0.2
5	3	3	6	2	3	56659	29407037.1	-1.1
10R30	29442483.3 MHZ					982.09553 CM-1		
9	1	-7	10	0	-7	29014	29442475.2	-8.1
9	1	-6	10	0	-6	33822	29442472.3	-11.0
9	1	-5	10	0	-5	40558	29442466.3	-17.0
9	1	-4	10	0	-4	50262	29442469.0	-14.3
8	2	8	9	1	8	9215	29442489.8	6.5
8	2	7	9	1	7	10497	29442486.3	3.0
8	2	6	9	1	6	12255	29442486.8	3.5
8	2	5	9	1	5	14701	29442486.1	2.8
8	2	4	9	1	4	18343	29442483.6	0.3
7	3	7	8	2	7	25530	29442482.1	-1.2
7	3	6	8	2	6	29733	29442481.5	-1.8
7	3	5	8	2	5	35560	29442478.7	-4.6
7	3	4	8	2	4	44194	29442474.8	-8.5
7	3	3	8	2	3	58435	29442482.0	-1.3
6	4	6	7	3	6	32116	29442473.9	-9.4
6	4	5	7	3	5	38205	29442468.4	-14.9
6	4	4	7	3	4	47093	29442468.8	-14.5
10R32	29477160.9 MHZ					983.25225 CM-1		
9	3	-9	10	2	-9	7221	29477141.5	-19.3
9	3	-8	10	2	-8	8152	29477138.8	-22.1
9	3	-7	10	2	-7	9345	29477136.4	-24.5
9	3	-6	10	2	-6	10903	29477136.4	-24.4
9	3	-5	10	2	-5	13117	29477134.5	-26.3
8	4	8	9	3	8	13563	29477147.3	-13.5
8	4	7	9	3	7	15488	29477147.3	-13.5
8	4	6	9	3	6	18092	29477152.3	-8.5
8	4	4	9	3	4	26929	29477148.9	-12.0
8	4	3	9	3	3	35536	29477144.5	-16.4
7	5	7	8	4	7	24549	29477150.8	-10.0
7	5	6	8	4	6	28493	29477146.5	-14.3
7	5	5	8	4	5	33982	29477150.7	-10.1
7	5	4	8	4	4	41910	29477146.2	-14.6

J"	K"	M"	J'	K'	M'	FIELD V/CM	VM(E) MHZ	VM(E)-VL MHZ
10R34	29511066.7 MHZ					984.38323 CM-1		
10	4	-10	11	3	-10	30755	29511030.1	-36.5
10	4	-9	11	3	-9	34090	29511039.7	-26.9
10	4	-8	11	3	-8	38412	29511036.6	-30.0
10	4	-7	11	3	-7	43970	29511034.4	-32.2
10	4	-6	11	3	-6	51334	29511037.0	-29.6
10	4	-5	11	3	-5	61971	29511025.3	-41.4
9	5	-9	10	4	-9	4579	29511045.2	-21.5
9	5	-8	10	4	-8	5158	29511044.5	-22.2
9	5	-7	10	4	-7	5883	29511046.0	-20.6
9	5	-6	10	4	-6	6872	29511045.5	-21.1
9	5	-5	10	4	-5	8223	29511048.0	-18.6
9	5	-4	10	4	-4	10321	29511046.5	-20.2
9	5	-3	10	4	-3	13849	29511044.8	-21.9
8	6	8	9	5	8	11587	29511065.9	-0.8
8	6	7	9	5	7	13221	29511065.7	-1.0
8	6	6	9	5	6	15377	29511063.9	-2.7
8	6	5	9	5	5	18398	29511065.7	-0.9
8	6	4	9	5	4	22837	29511065.2	-1.5
8	6	3	9	5	3	29966	29511061.5	-5.2
10R36	29544196.3 MHZ					985.48831 CM-1		
10	6	-10	11	5	-10	29847	29544184.5	-11.8
10	6	-9	11	5	-9	33194	29544186.2	-10.1
10	6	-8	11	5	-8	37392	29544188.8	-7.6
10	6	-7	11	5	-7	42823	29544191.7	-4.6
10	6	-6	11	5	-6	50184	29544191.4	-4.9
10	6	-5	11	5	-5	60708	29544188.9	-7.4
9	7	-9	10	6	-9	7901	29544186.5	-9.9
9	7	-8	10	6	-8	8873	29544190.0	-6.4
9	7	-7	10	6	-7	10098	29544197.0	0.7
9	7	-6	10	6	-6	11841	29544192.6	-3.7
9	7	-5	10	6	-5	14260	29544191.7	-4.6
9	7	-4	10	6	-4	17897	29544193.6	-2.7
10R38	29576545.1 MHZ					986.56735 CM-1		
14	3	14	15	2	14	10477	29576541.8	-3.3
14	3	13	15	2	13	11334	29576545.0	-0.2
14	3	12	15	2	12	12264	29576544.1	-1.0
14	3	11	15	2	11	13371	29576543.7	-1.4
14	3	10	15	2	10	14728	29576544.6	-0.5
14	3	9	15	2	9	16395	29576545.9	0.7
14	3	8	15	2	8	18427	29576545.1	-0.0
14	3	7	15	2	7	21072	29576545.4	0.3
14	3	5	15	2	5	29421	29576543.0	-2.2
14	3	6	15	2	6	24643	29576547.0	1.8
9	9	-6	10	8	-6	21972	29576516.3	-28.8
9	9	-5	10	8	-5	26571	29576517.0	-28.1
9	9	-4	10	8	-4	33765	29576513.3	-31.8
10R40	29608108.2 MHZ					987.62018 CM-1		
13	6	13	14	5	13	12198	29608114.8	6.7
13	6	12	14	5	12	13195	29608113.3	5.1
13	6	11	14	5	11	14413	29608115.0	6.9
13	6	10	14	5	10	15832	29608113.7	5.6
13	6	9	14	5	9	17587	29608113.9	5.7
13	6	8	14	5	8	19639	29608105.7	-2.4
13	6	7	14	5	7	22497	29608109.4	1.2
13	6	6	14	5	6	26189	29608108.2	0.0
13	6	5	14	5	5	31320	29608106.4	-1.8
10R42	29638880.2 MHZ					988.64663 CM-1		
13	8	-13	14	7	-13	16993	29638892.9	12.6
13	8	-12	14	7	-12	18326	29638902.2	22.0
13	8	-11	14	7	-11	20071	29638895.6	15.4
13	8	-10	14	7	-10	21998	29638903.7	23.5
13	8	-9	14	7	-9	24357	29638912.0	31.8
13	8	-8	14	7	-8	27426	29638912.7	32.5
12	9	12	13	8	12	5044	29638860.0	-20.2
12	9	11	13	8	11	5552	29638866.3	-14.0
12	9	10	13	8	10	6003	29638854.8	-25.4
12	9	9	13	8	9	6741	29638862.2	-18.0
12	9	8	13	8	8	7556	29638860.1	-20.1
12	9	7	13	8	7	8669	29638863.2	-17.1
12	9	6	13	8	6	10002	29638856.4	-23.8
12	9	5	13	8	5	12015	29638858.4	-21.8
12	9	4	13	8	4	14950	29638857.5	-22.7

Table 1b. Observed Stark shifted transitions using the $^{12}C^{18}O_2$ laser lines.

J"	K"	M"	J'	K'	M'	FIELD V/CM	VM(E) MHZ	VM(E)-VL MHZ
10R12	29241268.9 MHZ					975.38374 CM-1		
23	1	-23	23	0	-23	13705	29241263.3	-5.7
23	1	-22	23	0	-22	14319	29241263.6	-5.4
23	1	-21	23	0	-21	15009	29241263.3	-5.6
23	1	-20	23	0	-20	15761	29241263.3	-5.7
23	1	-19	23	0	-19	16603	29241263.0	-6.0
23	1	-18	23	0	-18	17532	29241262.8	-6.2
23	1	-17	23	0	-17	18538	29241263.4	-5.5
23	1	-16	23	0	-16	19698	29241263.4	-5.5
23	1	-15	23	0	-15	21025	29241263.1	-5.8
10R14	29277144.9 MHZ					976.58043 CM-1		
20	3	20	20	2	20	14198	29277141.6	-3.3
20	3	19	20	2	19	14950	29277141.8	-3.1
20	3	18	20	2	18	15772	29277141.5	-3.3
20	3	17	20	2	17	16707	29277141.8	-3.1
20	3	16	20	2	16	17748	29277141.7	-3.1
20	3	15	20	2	15	18935	29277141.9	-3.0
20	3	14	20	2	14	20285	29277141.9	-3.0
20	3	13	20	2	13	21843	29277141.9	-3.0
20	3	12	20	2	12	23668	29277142.0	-2.8
20	3	11	20	2	11	25828	29277142.3	-2.5
20	3	10	20	2	10	28410	29277142.5	-2.4
19	3	19	19	2	19	4069	29277142.9	-2.0
19	3	18	19	2	18	4294	29277142.8	-2.0
19	3	17	19	2	17	4547	29277142.8	-2.0
19	3	16	19	2	16	4836	29277143.0	-1.9
19	3	15	19	2	15	5156	29277142.9	-1.9
19	3	14	19	2	14	5524	29277142.9	-1.9
19	3	13	19	2	13	5961	29277143.3	-1.6
19	3	12	19	2	12	6429	29277142.5	-2.3
19	3	11	19	2	11	7037	29277143.1	-1.8
19	3	10	19	2	10	7741	29277143.1	-1.7
19	3	9	19	2	9	8600	29277143.1	-1.7
19	3	8	19	2	8	9681	29277143.2	-1.6
18	3	-18	18	2	-18	4636	29277144.2	-0.6
18	3	-17	18	2	-17	4910	29277144.2	-0.7
18	3	-16	18	2	-16	5215	29277144.2	-0.6
18	3	-15	18	2	-15	5562	29277144.3	-0.6
18	3	-14	18	2	-14	5961	29277144.2	-0.6
18	3	-13	18	2	-13	6429	29277143.9	-0.9
18	3	-12	18	2	-12	6959	29277144.1	-0.7
18	3	-11	18	2	-11	7596	29277144.0	-0.8
18	3	-10	18	2	-10	8354	29277144.1	-0.8
18	3	-9	18	2	-9	9286	29277144.0	-0.8
18	3	-8	18	2	-8	10442	29277144.1	-0.7
17	3	-17	17	2	-17	12016	29277144.8	-0.0
17	3	-16	17	2	-16	12773	29277144.6	-0.2
17	3	-15	17	2	-15	13636	29277144.2	-0.6
17	3	-14	17	2	-14	14593	29277144.9	0.0
17	3	-13	17	2	-13	15713	29277145.0	0.2
17	3	-12	17	2	-12	17031	29277144.8	-0.0
17	3	-11	17	2	-11	18583	29277144.8	-0.0
17	3	-10	17	2	-10	20435	29277145.1	0.3
17	3	-9	17	2	-9	22712	29277145.1	0.3
17	3	-8	17	2	-8	25565	29277145.1	0.2
16	3	-16	16	2	-16	18126	29277145.6	0.8
16	3	-15	16	2	-15	19336	29277145.7	0.8
16	3	-14	16	2	-14	20720	29277145.7	0.8
16	3	-13	16	2	-13	22309	29277146.0	1.1
16	3	-12	16	2	-12	24175	29277145.9	1.1
16	3	-11	16	2	-11	26386	29277145.7	0.9
16	3	-10	16	2	-10	28887	29277150.2	5.3
16	3	-9	16	2	-9	32271	29277145.9	1.0
10R16	29312217.6 MHZ					977.75033 CM-1		
18	5	18	18	4	18	27450	29312215.1	-2.4
18	5	17	18	4	17	29080	29312215.9	-1.6
18	5	16	18	4	16	30871	29312215.2	-2.3
18	5	15	18	4	15	32899	29312214.4	-3.1
17	5	17	17	4	17	18148	29312215.1	-2.4
17	5	16	17	4	16	19299	29312216.0	-1.6
17	5	15	17	4	15	20586	29312216.1	-1.4
17	5	14	17	4	14	22045	29312215.9	-1.7
17	5	13	17	4	13	23735	29312215.9	-1.7

J"	K"	M"	J'	K'	M'	FIELD V/CM	VM(E) MHZ	VM(E)-VL MHZ
10R16	29312217.6 MHZ					977.75033 CM-1		
16	5	16	16	4	16	10171	29312216.1	-1.4
16	5	15	16	4	15	10854	29312216.4	-1.2
16	5	14	16	4	14	11637	29312216.8	-0.8
16	5	13	16	4	13	12529	29312216.7	-0.8
16	5	12	16	4	12	13565	29312216.5	-1.0
16	5	11	16	4	11	14801	29312216.7	-0.8
16	5	10	16	4	10	16273	29312216.7	-0.9
15	5	15	15	4	15	3429	29312217.7	0.2
15	5	14	15	4	14	3675	29312217.8	0.2
15	5	13	15	4	13	3960	29312217.9	0.3
15	5	12	15	4	12	4285	29312217.7	0.1
15	5	11	15	4	11	4671	29312217.6	0.0
15	5	10	15	4	10	5142	29312217.7	0.2
15	5	9	15	4	9	5709	29312217.6	0.1
15	5	8	15	4	8	6416	29312217.5	-0.1
15	5	7	15	4	7	7342	29312217.7	0.2
14	5	-14	14	4	-14	2183	29312218.5	1.0
14	5	-13	14	4	-13	2351	29312218.5	0.9
14	5	-12	14	4	-12	2549	29312218.4	0.9
14	5	-11	14	4	-11	2780	29312218.4	0.9
14	5	-10	14	4	-10	3059	29312218.4	0.9
14	5	-9	14	4	-9	3429	29312217.4	-0.2
14	5	-8	14	4	-8	3826	29312218.4	0.8
14	5	-7	14	4	-7	4363	29312218.7	1.1
13	5	-13	13	4	-13	6729	29312219.1	1.6
13	5	-12	13	4	-12	7292	29312219.1	1.5
13	5	-11	13	4	-11	7946	29312219.6	2.0
13	5	-10	13	4	-10	8749	29312219.3	1.8
13	5	-9	13	4	-9	9716	29312219.7	2.1
13	5	-8	13	4	-8	10947	29312219.3	1.7
12	5	-12	12	4	-12	10271	29312220.5	2.9
12	5	-11	12	4	-11	11212	29312220.3	2.7
12	5	-10	12	4	-10	12343	29312220.0	2.5
12	5	-9	12	4	-9	13719	29312220.2	2.6
12	5	-8	12	4	-8	15433	29312220.7	3.1
12	5	-7	12	4	-7	17694	29312219.4	1.8
11	5	-11	11	4	-11	12913	29312220.7	3.1
11	5	-10	11	4	-10	14208	29312220.9	3.4
11	5	-9	11	4	-9	15795	29312221.1	3.6
11	5	-8	11	4	-8	17779	29312221.6	4.1
11	5	-7	11	4	-7	20349	29312221.7	4.1
11	5	-6	11	4	-6	23813	29312221.1	3.5
10	5	-10	10	4	-10	14700	29312221.7	4.1
10	5	-9	10	4	-9	16343	29312222.0	4.5
10	5	-8	10	4	-8	18378	29312223.9	6.4
10R18	29346485.3 MHZ					978.89338 CM-1		
18	7	18	18	6	18	39145	29346489.3	4.0
17	7	17	17	6	17	29002	29346489.5	4.2
17	7	16	17	6	16	30829	29346490.4	5.2
17	7	15	17	6	15	32872	29346490.5	5.2
17	7	14	17	6	14	35189	29346490.0	4.7
16	7	16	16	6	16	20264	29346492.5	7.3
16	7	15	16	6	15	21602	29346492.2	7.0
16	7	14	16	6	14	23111	29346491.2	5.9
16	7	13	16	6	13	24890	29346491.6	6.3
16	7	12	16	6	12	26966	29346492.2	6.9
16	7	11	16	6	11	29382	29346491.7	6.4
16	7	10	16	6	10	32327	29346492.8	7.5
16	7	9	16	6	9	35920	29346494.0	8.7
15	7	15	15	6	15	12740	29346493.6	8.3
15	7	14	15	6	14	13636	29346493.1	7.8
15	7	13	15	6	13	14692	29346493.6	8.3
15	7	12	15	6	12	15904	29346493.4	8.1
15	7	11	15	6	11	17345	29346493.5	8.2
15	7	10	15	6	10	19063	29346493.3	8.0
15	7	9	15	6	9	21193	29346494.2	8.9
15	7	8	15	6	8	23804	29346493.9	8.6
15	7	7	15	6	7	27163	29346494.0	8.7

Table 2a. Zero-field transitions of the observed lines using the $^{12}C^{16}O_2$ laser lines. RP 4 (12) denotes a $\Delta K = +1$, $\Delta J = -1$, $K = 4$;, $J = 12$ transition. * The lower member of the l doublett is observed.

TRANSITION	VM(O) MHZ	VM(O)-VL MHZ	LASER LINE
RP4(12)	28923750.0	703.7	10R 4
RP3(13)	28920521.0	-2525.6	10R 4
RP4(10)	28963791.0	-3666.5	10R 6
RP5(9)	28966923.0	-534.5	10R 6
RP6(8)	28969970.0	2512.9	10R 6
RP0(11)	29011069.0	-64.5	10R 8 *
RP1(8)	29054151.0	77.9	10R10
RP2(7)	29057338.0	3265.2	10R10
RP3(6)	29060495.0	6422.2	10R10
RQ3(15)	29177608.0	-847.7	10R16
RQ3(14)	29177886.0	-569.9	10R16
RQ3(13)	29178145.0	-311.1	10R16
RQ3(12)	29178385.0	-71.3	10R16
RQ3(11)	29178606.0	149.7	10R16
RQ3(10)	29178808.0	352.0	10R16
RQ3(9)	29178991.0	535.5	10R16
RQ3(8)	29179156.0	700.5	10R16
RQ3(7)	29179303.0	847.0	10R16
RQ3(6)	29179431.0	975.0	10R16
RQ3(5)	29179540.0	1084.7	10R16
RQ3(4)	29179632.0	1175.9	10R16
PP4(4)	29217985.0	-446.0	10R18
PQ4(16)	29294862.0	-1274.5	10R22
PQ4(15)	29295171.0	-965.8	10R22
PQ4(14)	29295460.0	-676.9	10R22
PQ4(13)	29295729.0	-407.7	10R22
PQ4(12)	29295978.0	-158.3	10R22
PQ4(11)	29296208.0	71.7	10R22
PQ4(10)	29296419.0	282.1	10R22
PQ4(9)	29296610.0	473.2	10R22
PQ4(8)	29296781.0	644.9	10R22
PQ4(7)	29296934.0	797.4	10R22
PQ4(6)	29297067.0	930.7	10R22
RR1(7)	29371436.0	606.0	10R26
RR0(6)	29368595.0	-2234.6	10R26 *
RR0(8)	29407990.0	-951.8	10R28 *
PR1(7)	29405001.0	-2037.8	10R28
PR2(6)	29402123.0	-4915.2	10R28
PR3(5)	29399252.0	-7786.4	10R28
PR1(9)	29444310.0	1826.4	10R30
PR2(8)	29441472.0	-1011.0	10R30
PR3(7)	29438641.0	-3842.4	10R30
PR4(6)	29435818.0	-6665.3	10R30
PR3(9)	29477946.0	785.2	10R32
PR4(8)	29475164.0	-1997.3	10R32
PR5(7)	29472389.0	-4771.5	10R32
PR4(10)	29514424.0	3356.7	10R34
PR5(9)	29511690.0	623.6	10R34
PR6(8)	29508963.0	-2104.1	10R34
PR6(10)	29548218.0	4021.3	10R36
PR7(9)	29545532.0	1335.2	10R36
PR3(14)	29575825.0	-720.4	10R38
PR9(9)	29579417.0	2872.0	10R38
PR6(13)	29606932.0	-1176.4	10R40
PR8(13)	29640793.0	1912.2	10R42
PR9(12)	29638187.0	-693.8	10R42

Table 2b. Zero-field transitions of the observed lines using the $^{12}C^{18}O_2$ laser lines.

TRANSITION	VM(O) MHZ	VM(O)-VL MHZ	LASER LINE
PQ1(23)	29241735.0	465.5	10R12
PQ3(20)	29276590.0	-554.8	10R14
PQ3(19)	29276977.0	-168.0	10R14
PQ3(18)	29277344.0	198.5	10R14
PQ3(17)	29277690.0	545.0	10R14
PQ3(16)	29278016.0	871.4	10R14
PQ5(18)	29311052.0	-1166.0	10R16
PQ5(17)	29311403.0	-814.7	10R16
PQ5(16)	29311734.0	-483.6	10R16
PQ5(15)	29312045.0	-172.6	10R16
PQ5(14)	29312336.0	118.3	10R16
PQ5(13)	29312607.0	389.4	10R16
PQ5(12)	29312858.0	640.6	10R16
PQ5(11)	29313090.0	872.2	10R16
PQ5(10)	29313302.0	1084.2	10R16
PQ7(18)	29344852.0	-1633.7	10R18
PQ7(17)	29345208.0	-1277.1	10R18
PQ7(16)	29345544.0	-941.0	10R18
PQ7(15)	29345860.0	-625.3	10R18
PQ7(14)	29346156.0	-329.9	10R18
PQ7(13)	29346431.0	-54.7	10R18
PQ7(12)	29346686.0	200.3	10R18
PQ7(11)	29346921.0	435.4	10R18
PQ7(10)	29347136.0	650.6	10R18
PQ7(9)	29347331.0	846.0	10R18
PQ7(8)	29347507.0	1021.6	10R18
RR18(23)	29380042.0	95.5	10R20
PQ9(17)	29379053.0	-893.3	10R20
PQ9(16)	29379395.0	-551.7	10R20
PQ9(15)	29379715.0	-230.9	10R20
PQ9(14)	29380016.0	69.3	10R20
PQ9(13)	29380295.0	349.0	10R20
PQ9(12)	29380555.0	608.2	10R20
PQ9(11)	29380793.0	847.2	10R20
PQ9(10)	29381012.0	1065.9	10R20

For the ground state we use the matrix elements (2), (5) and (6) with the corresponding ground state constants.

The energy matrix is set up for each state and each K, M-set ($K = |k|$) separately and diagonalized. For the excited state the matrix is offdiagonal in J, k and l. While the dimension of the matrix is finite in k and l, it is infinite in J. For diagonalisation the matrix was truncated at $J+10$, which gives the energy levels to the desired accuracy.

The parameters in Table 3 are obtained by a modified least-squares fit [30, 31] including 79 rotation-vibration transitions. For each transition we included a maximum of three M-components. The weight for each M-component is chosen such that each rotation vibration-transition had the same weight.

5. Discussion

As one may see from Table 1 or 2 much less P/R-branch than Q-branch transitions were assigned. This results from the facts that a) the chance for a laser line hitting a P/R-branch transi-

Table 3. Molecular Constants of CDF_3. The errors given are 2.5 times the standard deviation.

	0	ν_5	
$\nu°$	0.0	975.4317 (3)	cm^{-1}
$\nu°$	0.0	29242707.5 (8.4)	MHz
μ	1.6403 (26)	1.6499 (32)	Debye
B	9921.0318 [a]	9911.7382 [a]	MHz
C	5673.23 [b]	5672.48 (74)	MHz
D_J	0.0098 [a]	0.0102 (01)	MHz
D_{JK}	−0.0148 [c]	−0.0131 (25)	MHz
D_K	0.2218 (121) *	0.3312 (112) *	MHz
$(C\xi)$	—	4151.97 (1.15)	MHz
η_J	—	0.0263 (162)	MHz
η_K	—	−0.2027 (1163) *	MHz
q	—	0.6219	MHz

* These three parameters are significantly correlated. The errors given do not account for this correlation (see text).
[a] Ref. [20], [b] Ref. [21], [c] Ref. [32].

tion is significant less and b) P/R-branch lines usually have a much smaller Stark coefficient. Thus those lines are wider spread and appear in the saturation dip spectrum as broad and weak signals. On the other hand in the Doppler limited spectra they were covered by the strong and broad features originating from Q-branch transitions.

As a consequence of the position of the band centre we could observe 20 R-branch transitions and only 9 P-branch transitions. Therefore the parameters associated with the k quantum number-especially D_K'', D_K' and η_K — are determined less accurately than the others. The ground state parameter D_K'' can be evaluated by microwave spectroscopy only by observing $\Delta k = 3$ transition which was not done up to now. In addition the mentioned parameters are significantly correlated, so they could not be fitted at one. To derive suitable parameters we tried to fix D_K'' to zero. This led to an extreme hight value for η_K. Using the assumption $D_K'' = D_K'$, which is often used in IR spectroscopy, had nearly the same result with a much worse standard deviation

$$\sqrt{\sum_n |\nu_M(E) - \nu_L)^2]/n(n-1)}$$

of the fit (n in the number of lines included in the fit). Therefore we decided to fit each of the three parameters in separate calculations always keeping the other two fixed. The errors given in Table 3 are based on the figures evaluated in the separate fits. Since the correlation matrix is used to calculate these errors the values given do not account for the correlation of these three parameters.

As one may see from Table 1 the given parameters reproduce the assigned transitions quite well. The standard deviation of the fit is about 0.7 MHz with a maximum deviation of about 62 MHz for a single line.

Acknowledgements

We are very grateful to Dr. F. Winther for recording and analysing the IR-Fourier transform spectrum and for many helpful discussions. We would like thank Prof. Dr. H. Dreizler for his encouraging interest and for critical reading of the manuscript. We thank Prof. Dr. M. Winnewisser for placing his Fourier transform spectrometer at our disposal and M. Andolfatto for preparing a sample of CDF_3. The financial support of the Deutsche Forschungsgemeinschaft and the Fonds der Chemie is gratefully acknowledged. The calculations were carried out at the DEC PDP-10 Computer at the University Computation Centre.

[1] R. G. Brewer, M. J. Kelley, and A. Javan, Phys. Rev. Lett. **23**, 559 (1969).
[2] F. Shimizu, J. Chem. Phys. **52**, 3572 (1970); F. Shimizu, J. Chem. Phys. **53**, 1149 (1970).
[3] S. M. Freund, G. Duxbury, M. Römheld, J. T. Tiedje, and T. Oka, J. Mol. Spectrosc. **52**, 38 (1974).
[4] A. G. Maki and S. M. Freund, J. Mol. Spectrosc. **62**, 90 (1976).
[5] T. Tanaka, C. Yamada, and E. Hirota, J. Mol. Spectrosc. **63**, 142 (1976).
[6] G. Duxbury, S. M. Freund, and J. W. C. Johns, J. Mol. Spectrosc. **62**, 99 (1976); G. Duxbury and S. M. Freund, J. Mol. Spectrosc. **67**, 219 (1977).
[7] C. Yamada and E. Hirota, J. Mol. Spectrosc. **64**, 31 (1977).
[8] D. Coffey, C. Yamada, and E. Hirota, J. Mol. Spectrosc. **64**, 98 (1977).
[9] K. Kawaguchi, C. Yamada, T. Tanaka, and E. Hirota, J. Mol. Spectrosc. **64**, 125 (1977).
[10] K. Kawaguchi and T. Tanaka, J. Mol. Spectrosc. **68**, 125 (1977).
[11] M. Ieki, E. Kumamoto, K. Kawaguchi, C. Yamada, T. Tanaka, and E. Hirota, J. Mol. Spectrosc. **71**, 229 (1978).
[12] T. Amano and R. H. Schwendeman, J. Chem. Phys. **68**, 530 (1978).
[13] S. R. Polo and M. K. Wilson, J. Chem. Phys. **21**, 1129 (1953).
[14] L. C. Hoskins, J. Chem. Phys. **53**, 4216 (1970).
[15] A. Ruoff, H. Bürger, and S. Biedermann, Spectrochim. Acta **27A**, 1359 (1970).
[16] A. Ruoff, H. Bürger, and S. Biedermann, Spectrochim. Acta **27A**, 1377 (1970).
[17] A. Ruoff, H. Bürger, S. Biedermann, and R. Anttila, Spectrochim. Acta **31A**, 1099 (1975).

[18] N. J. Fyke, P. Lockett, J. K. Thomsen, and P. M. Wilt, J. Mol. Spectrosc. **58**, 87 (1975).
[19] S. N. Ghosh, R. Trambarulo, and W. Gordy, J. Chem. Phys. **20**, 605 (1952).
[20] C. C. Costain, J. Mol. Spectrosc. **9**, 317 (1962).
[21] W. L. Meerts and I. Ozier (1979): private communication.
[22] C. Freed and A. Javan, Appl. Phys. Lett. **17**, 53 (1970).
[23] C. Freed and R. G. O'Donnell, Metrologia **13**, 151 (1977).
[24] E. Ibisch, Diplomarbeit, Christian-Albrechts-Universität, Kiel 1978.
[25] F. Winther: private communication.
[26] F. R. Petersen, D. G. McDonald, J. P. Cupp, and B. L. Danielsen, in: Laser Spectroscopy, R. G. Brewer and A. Mooradien (editors), Plenum, Pupl. Corp., New York 1974, p. 555.
[27] C. Freed, A. H. M. Ross, and R. G. O'Donnell, J. Mol. Spectrosc. **49**, 439 (1974).
[28] H. C. Allen and P. C. Cross, Molecular Vib-Rotors, John Wiley, New York 1963, Chapter 4.
[29] G. J. Cartwright and I. M. Mills, J. Mol. Spectrosc. **34**, 415 (1970).
[30] D. W. Marquard, J. Soc. Indust. Appl. Math. **11**, 431 (1963).
[31] The subroutine used is based on a routine written by Veld at NRC/Ottawa.
[32] I. M. Mills, Spectrochim. Acta **19**, 1585 (1963).